Evolution of an optical vortex with an initial fractional topological charge

V. V. Kotlyar, A. A. Kovalev,* A. G. Nalimov, and A. P. Porfirev
Image Processing Systems Institute of the RAS—Branch of FSRC "Crystallography & Photonics" of the RAS, 151 Molodogvardeyskaya Street, Samara, 443001, Russia

(Received 22 April 2020; accepted 13 July 2020; published 12 August 2020)

In the general case, upon free-space propagation of a paraxial optical vortex (OV) its topological charge (TC) is not conserved, unlike the orbital angular momentum (OAM), which remains unchanged. In this work, we discuss a Gaussian beam with fractional TC in the source plane, showing theoretically and numerically in which way the TC is changing (but remains integer) upon free-space propagation. There are four evolution scenarios for an original OV with fractional TC that depend on how close the original TC is to an integer even or odd number. If the TC in the initial plane has an arbitrary fractional value, it becomes an odd integer in the Fourier plane. If the initial TC is close to an odd integer number, then, on propagation, an OV with a TC of +1 is born in the Fresnel diffraction zone, while in the far field an OV with a TC of –1 appears. This optical vortex with a TC of –1 is located in the beam periphery where the intensity is almost zero and thus it is difficult to detect it experimentally. Additional vortices with a TC of +1 and −1 are generated in the beam with the initial fractional TC due to the interference between a linear source appearing in the area of phase jump and an ordinary optical vortex with an integer TC. An experiment on registering the optical vortices by using the interferograms matches the theory and simulation. For simple OVs (such as Laguerre-Gaussian or Bessel-Gaussian modes), TC is conserved both upon propagation and following weak phase distortions. When scattered from a random phase screen, the integer TC of an OV is experimentally shown to conserve until random path-difference distortion reaches a half wavelength. Because of this, under weak-turbulence conditions, it makes sense to measure a discretely changing TC, rather than measuring the continuously varying OAM.

DOI: 10.1103/PhysRevA.102.023516

I. INTRODUCTION

Key characteristics of laser vortex beams [1] include topological charge (TC) and orbital angular momentum (OAM). Berry was the first to formulate the definition of the TC of an optical vortex (OV) [2], whereas the notion of OAM was introduced into optics in Ref. [3]. While the total OAM of a paraxial light field is conserved upon free-space propagation, the TC is sometimes conserved and sometimes not. The TC is conserved upon propagation if the amplitude of the original light field can be given by $E(r,\varphi) = A(r)\exp(in\varphi)$, where $A(r)$ is the amplitude constituent that depends only on the radial variable r, φ is the azimuthal angle, and n is the integer TC of OV. Examples of such light fields include the well-known Bessel-Gaussian and Laguerre-Gaussian beams. Examples of TC nonconservation upon OV propagation may be found in Refs. [4–9]. Simple superposition of a Gaussian beam and a Laguerre-Gaussian (LG) mode $(0, n)$ having different waist radius has been discussed [4]. Upon free-space propagation, total TC is changing due to different divergence of the constituent beams. If in the original plane the waist radius of the Gaussian beam is larger than that of the LG mode, total TC of superposition initially equals zero. Upon propagation, the difference between the waist radii decreases, with the waist radius of the LG mode at some point becoming larger than that of the Gaussian beam. From this point on, the TC of superposition becomes equal to n. Another example of nonconserving TC is described in [5], where the TC decreases with propagation distance after a circularly polarized beam passes through a slit with the shape of the Fermat spiral. It has been shown theoretically [2] and experimentally [6,7] that the original Gaussian beam with fractional TC has an integer TC in the near field, being equal to the nearest integer to the fractional number. However, it has been found that in the course of further propagation, the TC of the beams undergoes other, previously unknown changes. For instance, it has been numerically and experimentally shown [8] that, as it propagates as far as the Fresnel zone, the original OV with fractional TC is converted to an OV with an integer TC equal to the nearest integer to the original fractional TC plus 1. In a similar study conducted in Ref. [8], the TC was actually measured in the Fourier plane (focal plane of a spherical lens), producing results different from those reported in Ref. [9]. In [9], for a Gaussian OV $\exp(-r^2/w^2 + i\mu\varphi)$ with original fractional TC $\mu = (2k+1) + \varepsilon(0.1 < |\varepsilon| < 1)$, the far-field TC was shown to be $2k+1$. If the original fractional TC was $\mu = 2k + \varepsilon(0.1 < |\varepsilon| < 1)$, the far-field TC was also shown to be $2k+1$. The said studies have shown that, first, the TC is not always conserved on propagation and, second, even and odd TCs show a different stability towards changes. This conclusion can be drawn from the fact that regardless of the original fractional TC (close to an even integer or an odd integer) the far-field TC is always an odd integer.

We note that TC can be measured using a triangular diaphragm [10,11] or a cylindrical lens [12].

*alexeysmr@mail.ru

In this work, we study theoretically and numerically the evolution of a Gaussian beam with original fractional TC. We show that there are only four evolution scenarios for an OV with original fractional TC. We also show that the TC was measured in the near field in Refs. [2,6,7], in the Fresnel zone in [8], and in the far field in [9].

As a rule, an OV propagating in a turbulent atmosphere is identified by measuring its OAM [13,14]. However, due to minor "jitters" of both the entire laser beam and its constituent beams, there are continuous variations in OAM. For weak turbulence, OAM variations are small; otherwise they are strong. When measuring TC, we should bear in mind that it can only change discretely, while remaining integer. Hence, under weak turbulences, TC is not supposed to change at all. Analyzing the diffraction of an OV by a random phase screen, we show that TC remains unchanged until distortions of the random phase of the screen become essential.

II. THEORY

TC is calculated using a formula proposed by Berry [2]:

$$\mathrm{TC} = \frac{1}{2\pi} \lim_{r\to\infty} \mathrm{Im} \int_0^{2\pi} d\varphi \frac{\partial E(r,\varphi)/\partial\varphi}{E(r,\varphi)}. \tag{1}$$

The amplitude of a Gaussian beam with the original fractional TC is given by [2]

$$E(r,\varphi,z=0) = e^{-i\mu\varphi - r^2/w^2} = \frac{e^{i\pi\mu}\sin\pi\mu}{\pi} \sum_{n=-\infty}^{\infty} \frac{e^{in\varphi - r^2/w^2}}{\mu - n}. \tag{2}$$

In the Fresnel zone, the amplitude of field (2) is expressed as a difference of modified Bessel functions $I_\nu(x)$ [15]:

$$E(\rho,\theta,z) = \frac{\sin(\pi\mu)}{\sqrt{2\pi}} \left(\frac{-iz_0}{qz}\right) \times \exp\left(\frac{ik\rho^2}{2z} + i\pi\mu\right) \sqrt{x} e^{-x} \times \sum_{m=-\infty}^{\infty} (-i)^{|m|} \frac{e^{im\theta}}{\mu - m} \left[I_{\frac{|m|-1}{2}}(x) - I_{\frac{|m|+1}{2}}(x)\right], \tag{3}$$

where $x = (z_0/z)^2(\rho/w)^2/(2q)$, $q = 1 - i(z_0/z)$. Polar coordinates (r, φ) in Eqs. (1) and (2) are used for the initial plane $(z = 0)$, while for the field in other planes $(z > 0)$ we use in Eq. (3) and from now on the polar coordinates (ρ, θ).

In the near field $z \ll z_0$, the parameters in (3) take the form $x = ik\rho^2/(2z)$, $q = -i(z_0/z)$. Considering that the modified and conventional Bessel functions are connected as $I_\nu(ix) = i^\nu J_\nu(x)$, in the near field, we obtain [2,15]

$$E(\rho,\theta,z) = \frac{\sin(\pi\mu)}{\sqrt{2\pi}} \exp\left(\frac{ik\rho^2}{2z} + i\pi\mu\right) \sqrt{iy} e^{-iy} \times \sum_{m=-\infty}^{\infty} (-i)^{|m|} \frac{e^{im\theta}}{\mu - m} i^{(|m|-1)/2} \times \left[J_{\frac{|m|-1}{2}}(y) - iJ_{\frac{|m|+1}{2}}(y)\right], \tag{4}$$

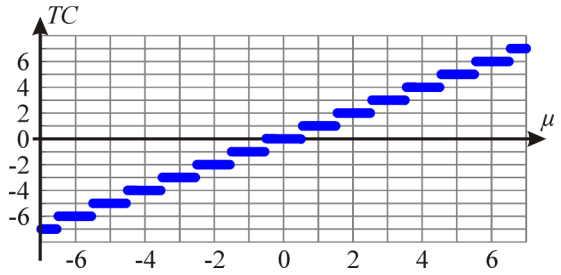

FIG. 1. TC in the near field for a Gaussian beam with the original fractional TC, calculated using Eq. (6).

where $y = k\rho^2/(2z)$. In the limit, at $\rho \to \infty$, using the asymptotic form of Bessel function $J_\nu(y \gg 1) \approx [2/(\pi y)]^{1/2}\cos(y - \nu\pi/2 - \pi/4)$, we get

$$E(\rho\to\infty,\theta,z) \approx \frac{\exp(i\pi\mu)\sin(\pi\mu)}{\pi} \sum_{m=-\infty}^{\infty} \frac{\exp(im\theta)}{\mu - m}. \tag{5}$$

Expressions (5) and (2) are identical at $w \to \infty$. Substituting (5) in (1), we derive a relationship for calculating TC in the near field:

$$\mathrm{TC} = \frac{1}{2\pi}\mathrm{Re}\left\{\int_0^{2\pi} \left[\sum_{n=-\infty}^{\infty} \frac{ne^{in\varphi}}{\mu - n}\right]\left[\sum_{n=-\infty}^{\infty} \frac{e^{in\varphi}}{\mu - n}\right]^{-1} d\varphi\right\}. \tag{6}$$

Calculations with the aid of Eq. (6) produce a well-known step function to describe TC jumps at $\mu = n + 1/2$ (Fig. 1). Figure 1 depicts in which manner the TC of field (2) depends in the near field on the original fractional TC μ, with calculations based on Eq. (6) conducted on the interval $-7 \leqslant \mu \leqslant 7$ with a 0.05 increment. It can be seen from Fig. 1 that the TC jumps occur at half-integer values, i.e., at $\mu = n + 0.5$, which is in agreement with Ref. [2].

Next, we calculate the TC in the Fresnel zone for the field with the original fractional TC of Eq. (2). Here, we can use the asymptotic form of the modified Bessel function at large argument values: $I_{(n-1)/2}(\xi) - I_{(n+1)/2}(\xi) \sim ne^\xi/[2\xi(2\pi\xi)^{1/2}]$ (it can be derived by using the expression 9.7.1 in [16]). Therefore, Eq. (3) is be reduced to

$$E(\rho\to\infty,\theta,z) = \left(\frac{-iz}{z_0}\right)\left(\frac{w}{\rho}\right)^2 \sin(\pi\mu) \times \exp\left(\frac{ik\rho^2}{2z} + i\pi\mu\right) \times \sum_{m=-\infty}^{\infty} (-i)^{|m|} \frac{\exp(im\theta)}{\mu - m} |m|. \tag{7}$$

Substituting (7) into (1), we obtain

$$\mathrm{TC} = \frac{\mathrm{Re}}{2\pi} \int_0^{2\pi} \left[\sum_{n=-\infty}^{\infty} \frac{(-i)^{|n|} n|n| e^{in\varphi}}{\mu - n}\right] \times \left[\sum_{n=-\infty}^{\infty} \frac{(-i)^{|n|}|n| e^{in\varphi}}{\mu - n}\right]^{-1} d\varphi. \tag{8}$$

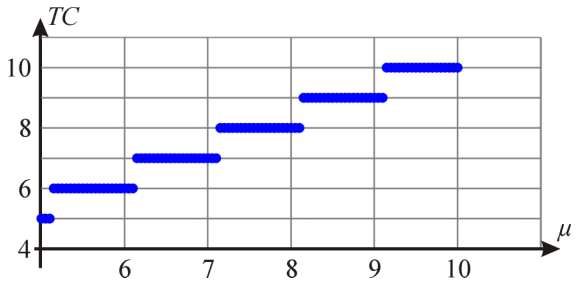

FIG. 2. TC in the Fresnel zone for a Gaussian beam with original fractional TC, Eq. (2), calculated using Eq. (8).

Figure 2 depicts the TC of a Gaussian beam with the original fractional TC of Eq. (2) calculated for the Fresnel diffraction zone using Eq. (8) for $5 \leqslant \mu \leqslant 10$ with a 0.05 step. From Fig. 2, the TC jumps are seen to be found near every integer number, when $\mu \approx n + 0.1$, which is in agreement with Ref. [8]. However, according to Ref. [8] such a pattern was characteristic of the Fraunhofer diffraction zone, rather than Fresnel zone. However, a similar study of TC of an OV in the far field (specifically, in the Fraunhofer diffraction zone or in the focus of a spherical Fourier lens) was conducted in Ref. [9], producing a different result.

In the far field (the focus of a Fourier lens), the amplitude of a light field takes the form

$$E_F(\rho,\theta) = \frac{\sin(\pi\mu)}{\sqrt{2\pi}}\left(\frac{-iz_0}{f}\right)\exp(i\pi\mu)\sqrt{x}\exp(-x) \times \sum_{m=-\infty}^{\infty}(-i)^{|m|}\frac{e^{im\theta}}{\mu-m}\left[I_{\frac{|m|-1}{2}}(x) - I_{\frac{|m|+1}{2}}(x)\right], \tag{9}$$

where the argument of Bessel functions is a real value: $x = (z_0/f)^2(\rho/w)^2/2$, and f is the focal length of a lens that generates the far field in the back focal plane. The calculation of TC using Eqs. (9) and (1) gives a step function shown in Fig. 3, which depicts the far-field TC of a Gaussian beam with the original fractional TC, Eq. (2), calculated using Eqs. (9) and (1) for $-5 \leqslant \mu \leqslant 5$ with a step of 0.05. From Fig. 3, jumps between adjacent integer values of TC occur at even integers, in agreement with Ref. [9].

Figures 1–3 suggest that the source field with original fractional TC [Eq. (2)] undergoes an interesting evolution. From Fig. 3 it is seen that in the far field, any original

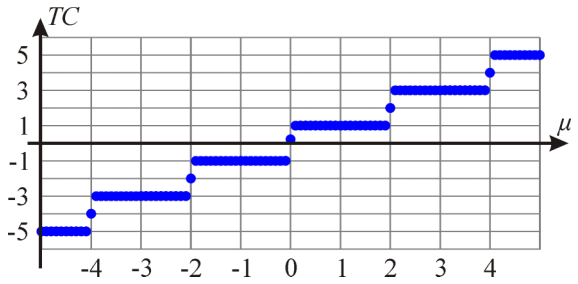

FIG. 3. Fourier-plane TC of a Gaussian beam with the original fractional TC, Eq. (2), calculated using Eqs. (9) and (1).

TABLE I. TC evolution scenarios on propagation of a Gaussian beam with the original fractional TC, $\exp(-r^2/w^2 + i\mu\varphi)$ (p is an arbitrary integer, $0 < \varepsilon < 1/2$).

Original TC ($z = 0$)	TC ($z \ll z_0$)	TC ($z \approx z_0$)	TC ($z \gg z_0$)
$\mu = 2p + \varepsilon$	$2p$	$2p+1$	$2p+1$
$\mu = 2p - \varepsilon$	$2p$	$2p$	$2p-1$
$\mu = (2p+1) + \varepsilon$	$2p+1$	$2p+2$	$2p+1$
$\mu = (2p+1) - \varepsilon$	$2p+1$	$2p+1$	$2p+1$

fractional field evolves to one that has only odd TCs. In the far field, the even TC can be generated only if the original field has an even integer TC. Actually, we assume that in the original plane the TC is $\mu = 3.3$. Then, in the near field, an OV with TC = 3 will be generated (Fig. 1); farther in the Fresnel zone, a new OV with TC of +1 will be born, with the total TC of the beam becoming equal to TC = 4 (Fig. 2). Meanwhile, in the far field another optical vortex with a TC of −1 will be born, with the total TC of the beam being again TC = 3 (Fig. 3), as in the near field.

The evolution of a field whose original fractional TC is closer to an even integer (e.g., $\mu = 4.3$) follows a different path. In the near field, the beam has TC = 4 (Fig. 1); in the Fresnel zone, TC = 5 (Fig. 2), with TC remaining unchanged in the far field, TC = 5 (Fig. 3).

There are two more evolution scenarios for a field with the original fractional TC, which can be seen from Table I, which gives all four feasible evolution scenarios for the initial fractional vortex. If a simple field has an integer TC in the source plane, TC is conserved during propagation. But this is not always the case. For a linear combination of two differently diverging light fields, the original integer TC will change upon propagation [4].

III. NUMERICAL SIMULATION

The numerical simulation aims to corroborate the values of TC derived from Eqs. (6), (8), and (9) for different diffraction zones of a Gaussian beam with the original fractional TC. The intensity and phase patterns in the near field and Fresnel zone are modeled by the Beam Propagation Method method (BEAMPROP software by RSoft) for the following parameters: wavelength $\lambda = 532$ nm, Gaussian beam waist $w_0 = 5\lambda(z_0 \sim 25\pi\lambda)$, initial TC $\mu = 3.3$, half size of the computational domain $R = 50\lambda$, transverse discretization step $\Delta x = \Delta y = \lambda/32$, and longitudinal discretization step $\Delta z = \lambda/16$. Meanwhile the amplitude and phase patterns in the far field are numerically modeled using a Fourier transform implemented with a spherical lens of focal length $f = 100$ mm for a Gaussian beam with waist radius $w_0 = 0.5$ mm and the same original TC $\mu = 3.3$ in the computational domain with the size of $2R = 1$ mm (the evolution scenario corresponds to line 4 of Table I). The patterns were calculated for a distance of $z = 3\lambda$ in the near field and $z = 50\lambda$ in the Fresnel zone.

Shown in Fig. 4 are the intensity (a–c) and phase (d–f) patterns for a Gaussian beam containing a fractional OV with $\mu = 3.3$ in the near field ($z = 3\lambda$) (a,d), Fresnel zone ($z = 50\lambda$) (b,e), and far field (in the Fourier plane of a focal

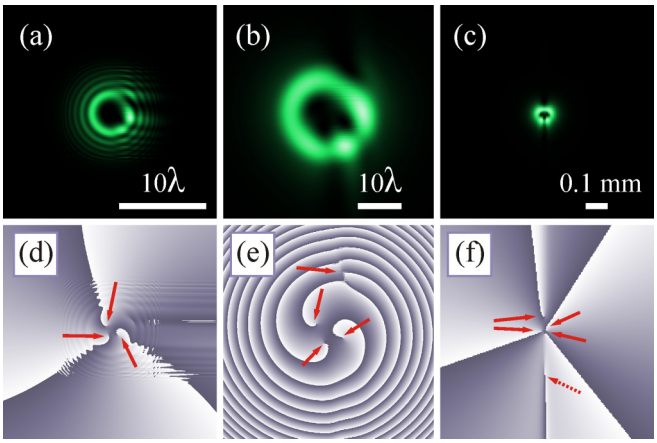

FIG. 4. Intensity (a–c) and phase (d–f) of a Gaussian beam with original fractional TC, $\mu = 3.3$ in the near field (a,d), Fresnel zone (b,e), and far field (c,f). Arrows in the phase distribution patterns mark OVs of the +first order, with a dashed arrow marking an OV of the –first order (f). Dark color denotes a zero phase and white is for a phase of 2π.

lens with focal length $f = 100$ mm) (c,f). Arrows in the phase distribution patterns mark optical vortices (singularity centers) of the +first order, with a dashed arrow in Fig. 4(f) marking an OV of –first order.

Figure 4 corroborates the calculation results derived from Eqs. (6), (8), and (9), which are depicted in Figs. 1–3, respectively, also corroborating the evolution scenario depicted in line 4 of Table I. Actually, from Fig. 4(d) it is seen that while in the source plane ($z = 0$) TC is $\mu = 3.3$, immediately behind it, at a distance of 3λ, there are only three singularity points and TC is $\mu = 3$. Although some phase distortions are present on the right in Fig. 4(d), no new singularity points can be seen. In Fig. 4(e) at a distance of 50λ (while the Rayleigh range is

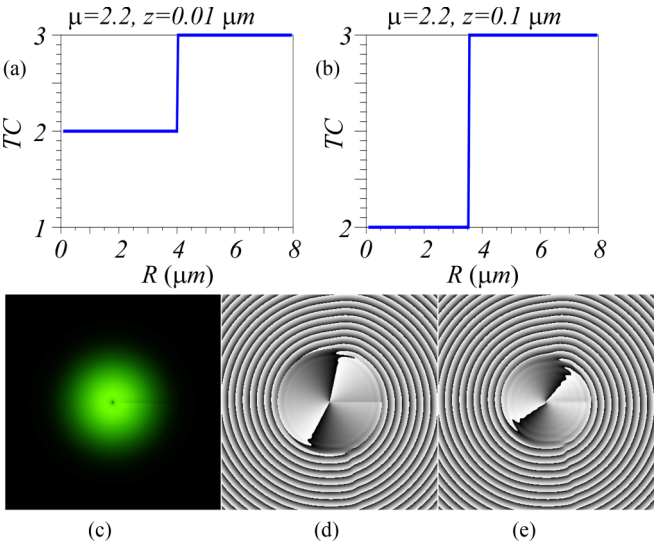

FIG. 5. Dependence of the beam TC on the radius R for the initial beam with $\mu = 2.2$ in the near field at distances $z = 0.01\,\mu$m (a) and $z = 0.1\,\mu$m (b); amplitude (c) and phase (d) at the distance $z = 0.01\,\mu$m and phase (e) at the distance $z = 0.1\,\mu$m.

75λ) a fourth singularity point is seen to form, as is evident from a fringe dislocation for three original singularity points, with TC being $\mu = 4$. Propagating further, the beam is seen to form one more singularity point of the opposite sign (–1) in the focus of a spherical lens [Fig. 4(f), bottom]. This brings the total TC of the beam back to the initial TC of $\mu = 3$.

Below we investigate in more detail how the additional optical vortices are born and propagate. Figure 5 shows the TC dependence on the radius R for the initial TC of $\mu = 2.2$ in the near field at distances of $z = 0.01\,\mu$m and $z = 0.1\,\mu$m. We use the following parameters of the field (2) in Fig. 5 (and below, in Figs. 6–8): field size 8 × 8 μm (400 × 400 points), wavelength $\lambda = 0.532\,\mu$m, Gaussian beam waist radius $w = 1.3\,\mu$m, and Rayleigh distance $z_R = \pi\omega_0^2/\lambda = 9.98\,\mu$m. According to Fig. 5, TC in the near field is equal to 3, starting from the radius $R > 4\,\mu$m. It is also seen that the phase of the field at distances of $z = 0.01\,\mu$m and $z = 0.1\,\mu$m remains the same in the whole field excepting the central area $R < 4.5\,\mu$m. Therefore, for the initial TC $\mu = 2.2$, TC of the optical vortex in the near field at the distance of just $z = 0.01\,\mu$m is equal to 3. Why does this simulation contradict the experiments in [6,7,10–12]? The answer is that, according to Fig. 5(c), intensity of the optical vortex decays almost to zero in the circle with the radius of nearly 2 μm, whereas the radius R of the circle where TC changes from 2 to 3 is about 4 μm. Thus, the additional singularity center is located in the area where it cannot be detected experimentally. Indeed, in Fig. 5 at $z = 0.1\,\mu$m and $\mu = 2.2$, the intensity on the circle where TC jumps from 2 to 3 ($R = 3.5\,\mu$m) equal 2.0×10^{-6} of its maximal value. Such low intensity cannot be measured experimentally.

Figure 6 shows that when the fractional part of the initial TC increases, the radius of the circle of the TC jump from 2 to 3 decreases. Therefore, for an optical vortex (2) with the initial fractional TC in the range $2.12 < \mu < 3$, TC in the Fresnel diffraction zone is equal to 3. The plot in Fig. 6 shows yet another interesting feature. If we suppose that R is the distance from the center of the field (i.e., of the Gaussian beam) to the third singularity, then with increase of the fractional part of the initial TC from 0.15 to 0.95 the third singularity is approaching from the periphery (where the intensity is almost

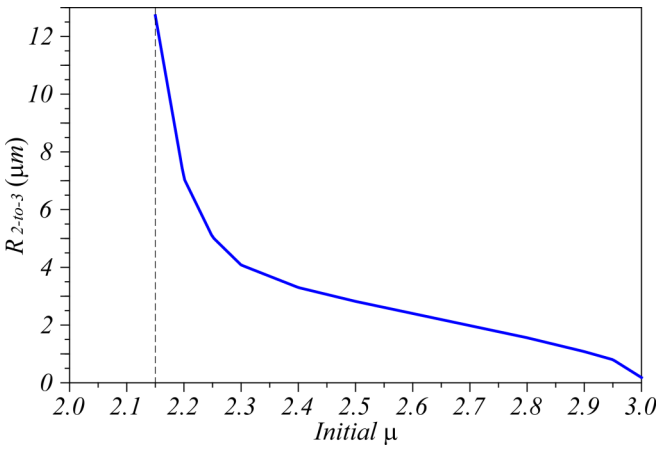

FIG. 6. Radius R where TC jumps from 2 to 3 vs the initial TC μ at $z = 10\,\mu$m.

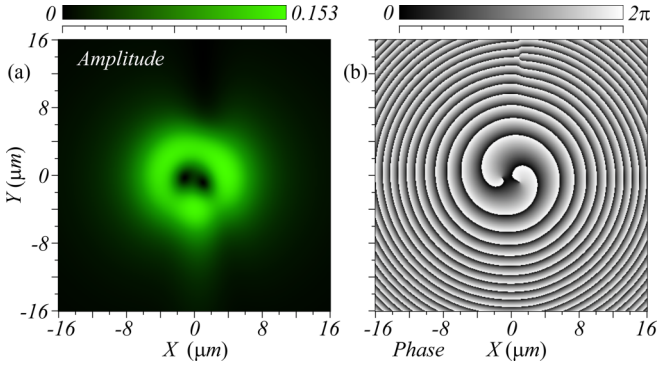

FIG. 7. Amplitude (a) and phase (b) of the field (2) with the initial TC $\mu = 2.2$ at the distance of $z = 20\,\mu$m (far field).

zero and thus cannot be detected) to the Gaussian beam center. Starting from a TC nearly of 2.5, it achieves the distance of circa 3 μm where the intensity can be measured and thus reveal this singularity. Therefore, the plot in Fig. 6 explains why in the experiments [6,7,10–12], the TC jumps from 2 to 3 at the fractional part of the initial TC are equal to 0.5. We note that for the initial fractional TC in the range from 3.1 to 4 we obtained a plot similar to Fig. 6. Therefore, we can claim that the plot similar to Fig. 6 is valid for arbitrary TC in the range $m < \mu < (m+1)$ (m is an arbitrary integer). In fact, our study made the bridge between the results of the work reported in Ref. [2] (TC jumps from m to $m+1$ when the fractional part is 0.5) and of the work reported in Ref. [8] (TC jumps at any fractional part).

Figure 7 shows amplitude and phase distributions of the initial field (2) at a distance of $z = 20\,\mu$m. The initial field has TC $\mu = 2.2$; its size is 32×32 μm (400×400 points). As seen in Fig. 7(b), there is a fork in the phase distribution (in the top of the figure) at a distance of about $R = 14\,\mu$m. Starting from this fork, the TC of the optical vortex changes from 2 to 3. Comparison of amplitude and phase in Fig. 7 reveals that the fork (third vortex) is in the beam periphery where the intensity is almost zero.

Where do the additional vortices come from? How are they born? Figure 8 illustrates phases of the field (2) in the near field for the different initial fractional TCs: $\mu = 2.11$, $z = 1\,\mu$m [Fig. 8(a)], $\mu = 2.2$, $z = 0.1\,\mu$m [Fig. 8(b)], and $\mu = 2.4$, $z = 1\,\mu$m [Fig. 8(c)]. As seen in Fig. 8, there are two screw dislocations on the phase distributions in the very center of the beam and one edge dislocation (distorted fringes) in the top phase area [Fig. 8(a)], or in the bottom area [Figs. 8(b) and 8(c)]. This edge dislocation appears due to the interference of an optical vortex with TC = 2 and of a boundary wave propagating from the area of the phase break [horizontal dark line in Fig. 5(a)]. On further propagation, this edge dislocation leads to a screw dislocation [additional optical vortex or fork in Fig. 7(b)].

Yet another question arises as to whether TC in the far field is always odd for any fractional μ. Figure 9 depicts phases for the field (2) with the waist radius $w = 0.5$ mm in the rear focal plane of a spherical lens with the focal length $f = 100$ mm for different values of μ: 2.3 [Fig. 9(a)], 3.3 [Fig. 9(b)], 4.2 [Fig. 9(c)], and 5.1 [Fig. 9(d)]. As seen in Fig. 9 for an even integer $m = 2$ [Fig. 9(a)], in addition to two initial vortices there is an additional third vortex in the top area, while in the bottom area there is no vortex (i.e., TC = 3). At the even value $m = 4$ [Fig. 9(c)], besides the initial four vortices there is an additional fifth vortex in the top area and there is no vortex in the bottom area (i.e., TC = 5). In the bottom areas of Figs. 9(a) and 9(c), there is a line of phase jump by 2π. For odd values $m = 3$ [Fig. 9(b)] and $m = 5$ [Fig. 9(d)], the additional vortex at the top is compensated by the additional vortex at the bottom. Therefore, TC is equal to 3 in Fig. 9(b) and 5 in Fig. 9(d).

As seen in Fig. 9, additional optical vortices with a TC of $+1$ (at the top) and with a TC of -1 [at the bottom of Figs. 9(b) and 9(d)] are located far from the beam center and these distances are not equal. The vortices with a TC of -1 are farther than the vortices with a TC of $+1$. The distance from the center to the vortex does not affect the TC of the whole beam, but it affects the results of the experiment. Both vortices ($+1$ and -1) are located at the distance from the beam center where the intensity is almost zero. Therefore, they are hard to register experimentally.

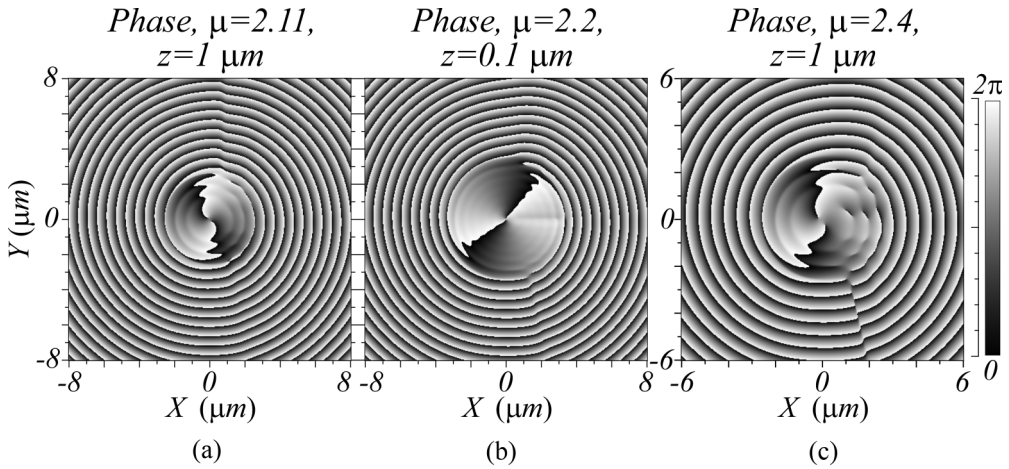

FIG. 8. Phases of the field (2) with the different initial TCs in the near field: $\mu = 2.11$, $z = 1\,\mu$m (a), $\mu = 2.2$, $z = 0.1\,\mu$m (b), $\mu = 2.4$, $z = 1\,\mu$m (c).

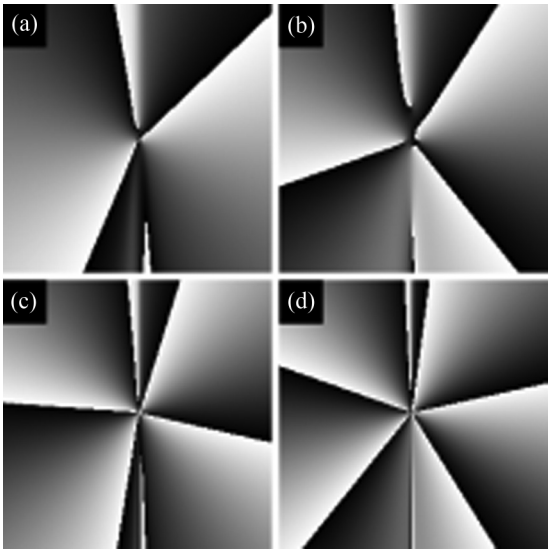

FIG. 9. Phases of the field (2) with the waist radius $w = 0.5$ mm in the focus of the spherical lens ($f = 100$ mm) for different values of μ: 2.3 (a), 3.3(b), 4.2 (c), 5.1 (d).

IV. EXPERIMENT

Figure 10 shows the experimental setup used in the experiments. A linearly polarized Gaussian laser beam ($\lambda = 532$ nm; w_0 is approx. 5 mm) was expanded and collimated with a combination of a pinhole PH (with an aperture of 40 μm) and a lens L1 with a focal length of 350 mm. The mirrors M1 and M2 as well as two beam splitters B1 and B2 were used to implement the Mach-Zehnder interferometric setup. The collimated laser beam was normally incident on the display of the spatial light modulator SLM (Holoeye LC-2012, 1024 × 768 pixels), which was used for the implementation of the phase transmission function of the elements generating the Gaussian beam with the original fractional TCs of 2.2, 2.7, 3.3, and 3.7. The 4-f optical system consisted of the lenses L2 (focal length $f_2 = 150$ mm) and L3 (focal length $f_3 = 150$ mm), and a diaphragm D spatially filtered the laser beam generated by the SLM. The intensity pattern formed in the near field, Fresnel zone, and focal plane of the lens L4 (focal length $f_4 = 350$ mm) was recorded with a video camera camera Cam (3264 × 2448 pixels, 1.67-μm pixel size). A neutral density filter F was used to equalize the intensities of the object and the reference beams.

Figure 11 shows the intensity and interferogram patterns obtained in the experiments.

The topological charge of the optical vortices from Fig. 11 is given in Table II. It is obtained by simply counting the "fork teeth" on the interferograms in Fig. 11.

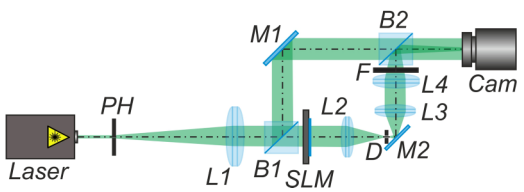

FIG. 10. Experimental setup for investigation of TCs of the generated OVs.

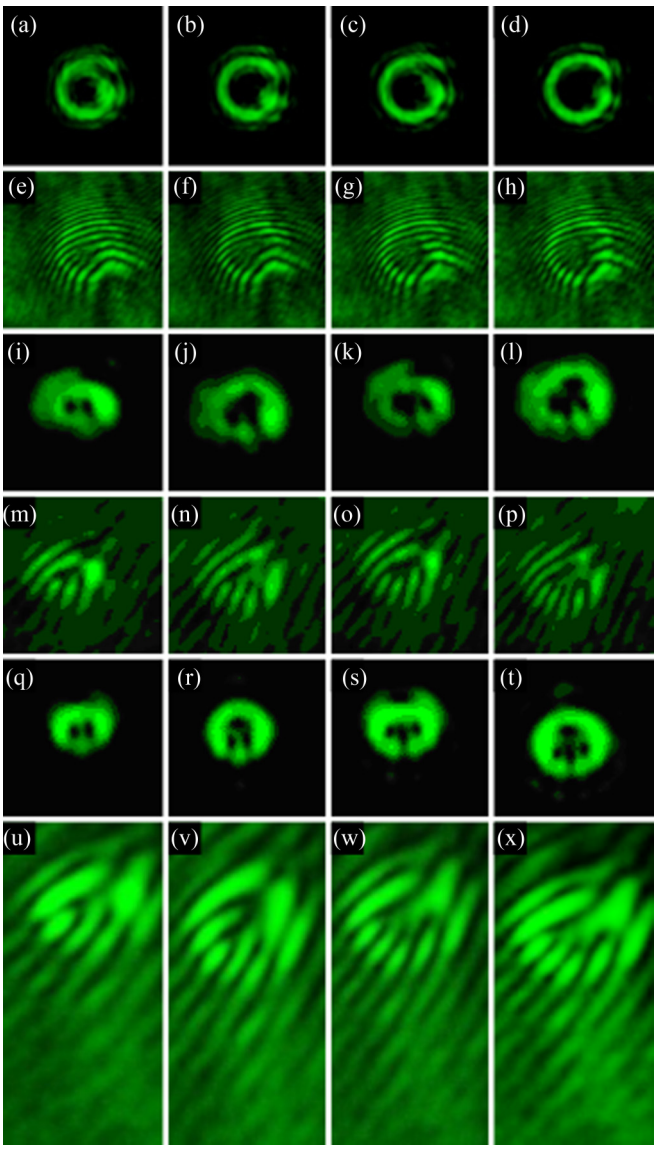

FIG. 11. Intensity (a–d,i–l,q–t) and interferogram (e–h,m–p,u–x) patterns obtained in the case of a Gaussian beam with the original TCs μ: 2.2 (a,e,i,m,q,u), 2.7 (b,f,j,n,r,v), 3.3 (c,g,k,o,s,w), and 3.7 (d,h,l,p,t,x). The image size is 1100 × 1100 μm (a–h), 200 × 200 μm (i–t), 150 × 300 μm (u–x).

The third row of Table II contains TC values obtained from the interferograms [Figs. 11(e)–11(h)] of the optical vortices in the near field, whose intensity is shown in Figs. 11(a)–11(d). It is seen in the third row of Table II that in the near field (at a distance 40 mm from the focus of the lens L4 in Fig. 10) the experiment matches the theory (Fig. 1)

TABLE II. Experimental TC of different fractional optical vortices in different diffraction zones.

	Topological charge			
Initial field	2.2	2.7	3.3	3.7
Near field	2	3	3	4
Fresnel zone	3	3	4	4
Lens focus	3	3	3	3

and the simulation [Fig. 4(d)], but contradicts the simulation from Fig. 5. We gave an explanation for this contradiction above: The additional vortex in Fig. 5 for the initial TC of 2.2 is generated far from the optical axis and thus cannot be registered experimentally. The fourth row of Table II contains TCs in the Fresnel diffraction zone (at a distance of 4 mm from the focus of the lens L4 in Fig. 10). These values were measured from the interferograms [Figs. 11(m)–11(p)] for the optical vortices, whose intensity is shown in Figs. 11(i)–11(l). For the Fresnel zone, the TC from Table II coincides with the theory (2) and with the simulation in Figs. 4(e) and 6. The last (fifth) row of Table II contains TCs in the far field (in the focus of the spherical lens L4 in Fig. 10). These values were found from the interferograms [Figs. 11(u)–11(x)] of the optical vortices with intensity shown in Figs. 11(q)–11(t). The experimental results shown in the fifth row of Table II agree with the theory (3) and with the simulation in Figs. 4(f) and 9. Indeed, for an even integer part of the TC value $m = 2$, as seen in Figs. 11(u) and 11(v), the forks on the interferogram contain three additional teeth. For the odd integer part of the TC value $m = 3$, interferogram analysis in Figs. 11(w) and 11(x) is more complicated. In the beam center, there are four additional fork teeth clearly seen on the interferogram. However, in the bottom part of the interferogram, the characteristic defect of fringes can be seen (although with a low contrast), which reveals the additional vortex with a TC of -1. Therefore, for fractional vortices with the odd value $m = 3$, the TC in the far field equals 3. The weak contrast of fringes in the bottom parts of the interferograms is due to the low intensity in the beam periphery. Thus, in the far field, the experiment also confirms the theory (3) and the simulation in Figs. 4(f) and 9.

We also made an experimental study of the stability of an OV's TC against phase distortions. Specifically, we experimentally study the conservation of the integer TC following random phase distortions of a vortex laser beam. The experimental setup is similar to that in [17], but the phase distortions are generated on a spatial light modulator (SLM) instead of the ground glass plate, thus allowing us to change the distortion's magnitude and to define such threshold distortions for which TC is still conserved. We also adopt a more accurate method of TC measurement, using for this purpose a cylindrical lens [12]. A Gaussian beam with waist radius $w = 1.1$ mm is incident on a spatial light modulator, where a vortex phase $m\varphi$ with $m = 5$ is recorded. Each pixel of the SLM is being distorted by adding $2\pi\alpha$ to its phase $m\varphi$, where α is a random number from the interval [0, 1]. Figure 12 depicts distorted phases of the original light field recorded on the SLM (left column), intensity patterns (600 × 600 μm) measured in the focal plane of a spherical lens with focus $f = 150$ mm (central column), and intensity patterns (1900 × 1900 μm) measured at a double focal length from a cylindrical lens with focus $f = 100$ mm (right column) for different phase distortions α. In our experiment, we use the SLM (Holoeye LC-2012, 1024 × 768 pixels), with a pixel size of 8 μm. Random phase jumps on the SLM are seen as dark (phase is 0) and light (phase is 2π) dots in Figs. 12(d), 12(g), 12(j), 12(m), and 12(p). The phase on the SLM is changed in each pixel by a proportional changing of the refractive index of the liquid crystal. Therefore, the power spectrum

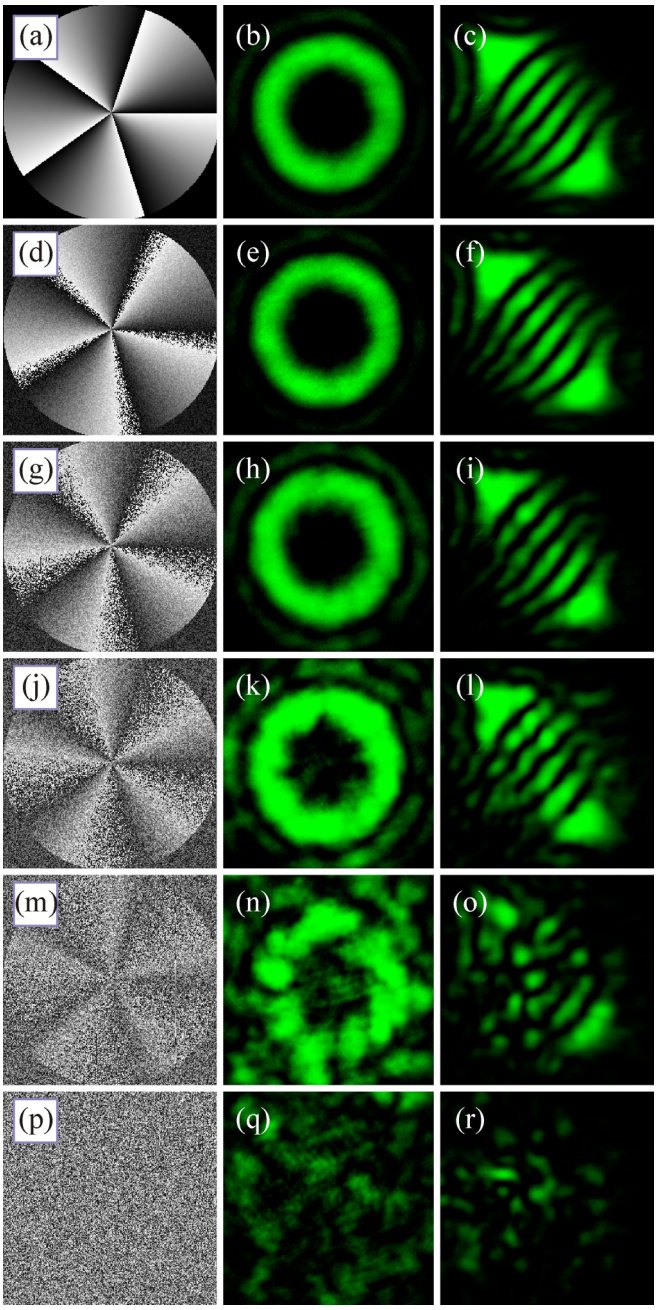

FIG. 12. Distorted phase patterns (a,d,g,j,m,p), intensity patterns (600 × 600 μm) in the focal plane of a spherical lens with focus $f = 150$ mm (b,e,h,k,n,q), and intensity patterns (1900 × 1900 μm) at a double focal length of a cylindrical lens with focus $f = 100$ mm (c,f,i,l,o,r) for different degrees of distortion: $\alpha = 0$ (a–c), $\alpha = 0.2$ (d–f), α=0.4 (g–i), α=0.6 (j–l), α=0.8 (m–o), and α=1.0 (p–r).

of the random phase distortions is not that of white noise. Instead, the correlation function of the distortions has the width defined by the SLM pixel size.

Figure 12 suggests that at $\alpha = 0.6$ (i.e., the phase is distorted by a random value from the interval $[0, 1.2\pi]$), six peaks are still clearly seen on the diagonal at an angle of $-45°$ (either five dark fringes or five intensity nulls), meaning that the optical vortices have a TC of 5. However, at $\alpha \geqslant 0.8$, TC is nowhere to be seen (Fig. 12). Therefore, the TC of

an optical vortex remains equal to the integer 5 until random phase distortion of the initial vortex gets as large as about a half wavelength ($\lambda/2$).

V. CONCLUSION

Summing up, it has been theoretically shown that a Gaussian beam with an embedded OV with original fractional TC does not conserve the original TC upon propagation. The TC of the Gaussian beam with the original fractional TC can take different values in different diffraction zones, such as near field ($z \ll z_0$), Fresnel zone ($z \approx z_0$), and far field ($z \gg z_0$) . This conclusion has been corroborated via numerical simulation using the BEAMPROP software for the near field and Fresnel zone and a Fourier transform for the far field. Four evolution scenarios for the fractional Gaussian beam have been described. In one scenario, if the source beam has a TC of 3.3, it has been shown to have a TC of 3 in the near field, a TC of 4 in the Fresnel zone, and again a TC of 3 in the Fraunhofer zone (in the focus of a spherical lens). Thus, in this evolution scenario, an OV with a TC of $+1$ is produced in the Fresnel zone, before being compensated for in the far field by a newly born OV with a TC of -1. The experiment on the determining TC by using the interferograms matches the theory and the simulation. We have also shown experimentally that given weak random phase distortions (a phase shift smaller than π), TC is conserved. Based on these properties, it becomes possible to identify OVs in wireless communications by measuring TC, alongside OAM measurements.

Additional OVs in the Fresnel and Fraunhofer diffraction zones (see Table I) are explainable since the initial fractional-TC light field contains the whole angular harmonics spectrum and thus carries all these additional OVs. Two well-known examples confirm this. If the Hermite-Gaussian beam of order $(0, n)$ passes in the initial plane through a cylindrical lens rotated by 45° to the Cartesian axes, its initial TC is zero. However, at the double focal length, the beam transforms to a vortex LG beam with the order $(0, n)$ [18]; i.e., an OV with TC of n was born. As another example, if in the initial plane there is a combined beam composed of a Gaussian beam with the waist radius w_1 and of a LG vortex with the order $(0, n)$ and waist radius w_2, and if $w_1(0) < w_2(0)$, then the TC of such combined beam equals n up to a distance z_1 [4]. At $z > z_1$, though, $w_1(z) > w_2(z)$ and TC becomes zero; i.e., n OVs were born with a TC of -1 and compensated n OVs with a TC of $+1$ that were present in the initial plane.

ACKNOWLEDGMENTS

This work was funded by the Russian Foundation for Basic Research Grants No. 18-29-20003 and No. 18-07-01129, Russian Science Foundation Grant No. 18-19-00595, and by RF Ministry of Science and Higher Education under the government project of FRDC for "Crystallography and Photonics" RAS.

[1] V. V. Kotlyar, A. A. Kovalev, and A. P. Porfirev, *Vortex Laser Beams* (CRC Press, Boca Raton, FL, 2018).

[2] M. V. Berry, Optical vortices evolving from helicoidal integer and fractional phase steps, J. Opt. A: Pure Appl. Opt. **6**, 259 (2004).

[3] L. Allen, M. Beijersbergen, R. Spreeuw, and J. Woerdman, Orbital angular momentum of light and the transformation of Laguerre-Gaussian laser modes, Phys. Rev. A **45**, 8185 (1992).

[4] M. S. Soskin, V. N. Gorshkov, M. V. Vastnetsov, J. T. Malos, and N. R. Heckenberg, Topological charge and angular momentum of light beams carrying optical vortex, Phys. Rev. A **56**, 4064 (1987).

[5] H. Wang, L. Liu, C. Zhou, J. Xu, M. Zhang, S. Teng, and Y. Cai, Vortex beam generation with variable topological charge based on a spiral slit, Nanophotonics **8**, 317 (2019).

[6] J. Leach, E. Yao, and M. J. Padgett, Observation of the vortex structure of a non-integer vortex beam, New J. Phys. **6**, 71 (2004).

[7] J. B. Gotte, S. Franke-Arnold, R. Zambrini, and S. M. Barnett, Quantum formulation of fractional orbital angular momentum, J. Mod. Opt. **54**, 1723 (2007).

[8] A. J. Jesus-Silva, E. J. S. Fonseca, and J. M. Hickmann, Study of the birth of a vortex at Fraunhofer zone, Opt. Lett. **37**, 4552 (2012).

[9] J. Wen, L. Wang, X. Yang, J. Zhang, and S. Zhu, Vortex strength and beam propagation factor of fractional vortex beams, Opt. Express **27**, 5893 (2019).

[10] J. M. Hickmann, E. J. S. Fonseca, W. C. Soares, and S. Chavez-Cerda, Unveiling a Truncated Optical Lattice Associated with a Triangular Aperture Using Lights Orbital Angular Momentum, Phys. Rev. Lett. **105**, 053904 (2010).

[11] A. Mourka, J. Baumgartl, C. Shanor, K. Dholakia, and E. M. Wright, Visualization of the birth of an optical vortex using diffraction from a triangular aperture, Opt. Express **19**, 5760 (2011).

[12] V. V. Kotlyar, A. A. Kovalev, and A. P. Pofirev, Astigmatic transforms of an optical vortex for measurement of its topological charge, Appl. Opt. **56**, 4095 (2017).

[13] G. Gibson, J. Courtial, M. J. Padgett, M. Vasnetsov, V. Pasko, S. M. Barnett, and S. Franke-Arnold, Free-space information transfer using light beams carrying orbital angular momentum, Opt. Express **12**, 5448 (2004).

[14] R. J. Watkins, K. Dai, G. White, W. Li, J. K. Miller, K. S. Morgan, and E. G. Jonson, Experimental probing of turbulence using a continuous spectrum of asymmetric OAM beams, Opt. Express **28**, 924 (2020).

[15] V. V. Kotlyar, A. A. Almazov, S. N. Khonina, V. A. Soifer, H. Elfstrom, and J. Turunen, Generation of phase singularity through diffracting a plane or Gaussian beam by a spiral phase plate, J. Opt. Soc. Am. A **22**, 849 (2005).

[16] M. Abramowitz and I. A. Stegun, *Handbook of Mathematical Functions*, Applied Mathematics Series No. 55 (National Bureau of Standards, Washington, DC, 1965).

[17] G. R. Salla, C. Perumangattu, S. Prabhakar, A. Anwar, and R. P. Singh, Recovering the vorticity of a light beam after scattering, Appl. Phys. Lett. **107**, 021104 (2015).

[18] E. G. Abramochkin and V. G. Volostnikov, Beam transformations and nontransformed beams, Opt. Commun. **83**, 123 (1991).